

# Preoperative local staging of gastric adenocarcinoma with 3D multi-detector row computerized tomography

Essay

Submitted for partial fulfillment of Master degree in Radiodiagnosis

By

Basma Saber Ibrahim Ali

M.B., B.Ch. Faculty of Medicine Ain Shams University

# Supervised By

#### **Dr. Sahar Mohamed El-Fiky**

Professor of Radio-diagnosis Faculty of Medicine Ain Shams University

#### Dr. Maha Abdel Meguid El-Shinnawy

Assistant professor of Radiodiagnosis Faculty of Medicine Ain Shams University

Radiodiagnosis Department Faculty of Medicine Ain Shams University 2013

**Acknowledgement** 

I would like to express my deep gratitude to Prof. Dr. Sahar Mohammed El-Fiky, Professor of Radiodiagnosis, Faculty of Medicine, Ain-Shams University, under whose supervision I had the honor to proceed with this work.

I wish to express supreme respect to Dr. Maha
Abdel Meguid El Shinnawy, Assistant professor of
Radiodiagnosis, Faculty of Medicine, Ain-Shams
University, for her continuous advice, and fruitful
criticism that made this work come to existence.

### **Contents**

Title	page
Introduction and aim of the work	
Basic and radiological anatomy of the stomach	
Basic anatomy of the stomach	3-10
Radiological anatomy and normal variations	11-21
Pathology of gastric adenocarcinoma	
Classification of gastric neoplasms	22
Adenocarcinoma	23-29
Technique of 3D multidetector CT	
Patient preparation	30-31
Patient position	31
CT protocol	31-32
Post processing	32-35
Limitations of the study	35-36
CT findings in gastric adenocarcinoma	
CT appearance of gastric adenocarcinoma	37-41
Perigastric invasion	41-43
Nodal spread	44-45
Distant metastasis	45-48
Sensitivity of multidetector row CT in gastric	49-50
adenocarcinoma detection	
Virtual gastroscopy versus conventional gastroscopy	51-53
Illustrative cases	
case 1	54
case 2	55
case 3	56-57
case 4	58-59
case 5	60
case 6	61
Summary and conclusion	62-64
References	65-71
Arabic summary	72-76

# **List of abbreviations**

US	Ultrasonography			
CT	Computed tomography			
MDCT	Multidetector computed tomography			
MPRs	Multiplanar reformations			
EGC	Early gastric cancer			
TNM	Tumor, node, metastasis			
SSD	Surface shaded display			
MA	Milliampere			
KV	Kilovolt			
3D CT	Three dimensional computed tomography			
VR	Volume rendering			
LOCM	Low osmolar contrast medium			

# **List of figures**

Figure	Title	Page
Fig.1.1	Anatomy of the stomach.	3

Fig. 1.2	Parts of the stomach.	4
Fig. 1.3	Muscle layers of the stomach	5
Fig. 1.4	Relations of the stomach.	6
Fig. 1.5	Stomach bed.	6
Fig. 1.6	Arterial blood supply of the stomach.	8
Fig. 1.7	Venous drainage of the stomach.	8
Fig. 1.8	Lymphatic drainage of the stomach.	9
Fig. 1.9	Nerve supply of the stomach.	10
Fig. 1.10	CT appearance of gastroesophageal junction.	12
Fig. 1.11	CT appearance of the pylorus.	13
Fig. 1.12	Axial CT scan of the abdomen with oral and IV	14
	contrast.	
Fig. 1.13	Axial CT scan of the abdomen with oral and IV contrast	15
	showing metastatic lymphadenopathy.	
Fig. 1.14	Coronal CT scan with oral and IV contrast showing an	16
	exophytic gastric carcinoma	
Fig. 1.15	Axial CT scan of the abdomen with oral and IV contrast	<b>18</b>
	showing normal stomach position.	
Fig. 1.16	Axial CT scan of the abdomen with oral and IV contrast	18
	showing relations of the fundus of the stomach.	
Fig. 1.17	Axial CT scan of the abdomen with oral and IV contrast	19
	showing relations of the stomach body.	
Fig. 1.18	Axial CT scan of the abdomen with oral and IV contrast	19
71 110	showing relations of the stomach body and antrum.	•
Fig. 1.19	Axial CT scan of the abdomen with oral and IV contrast	20
Ti 4.00	showing relations of the stomach body and antrum.	•
Fig. 1.20	Axial CT scan of the abdomen with oral and IV contrast	20
Ti 4 04	showing relations of the stomach body and antrum.	
Fig. 1.21	MPR image of air-filled stomach in the venous phase of	21
	triphasic multidetector CT (MDCT) of abdomen.	
Fig. 2.1(a)	CT costus quarkie images of CA cross ald mass in 200 LBO	24
Fig. 3.1(a)	CT gastrographic images of 64-year-old man in 30° LPO	34
Fig. 2.1(b)	position.  CT costrography image of stomach in left nesterior	24
Fig. 3.1(b)	CT gastrography image of stomach in left posterior	34
	oblique position resulting from use of volume-rendering	
Eig 2.2	technique.	24
Fig. 3.2	3D examination of the stomach, reconstructed images of	34

	helical CT of the stomach showing all stomach parts.		
Fig. 3.3	3D examination of the stomach, reconstructed images of	35	
	helical CT of the stomach showing all stomach parts.		
Fig. 4.1	Coronal reformatted CT scan of the abdomen after oral	38	
	and IV contrast showing a type IIa tumor.		
Fig. 4.2	Coronal reformatted CT scan of the abdomen after oral	38	
	and IV contrast showing focal wall thickening in the		
	antrum with marked enhancement of the mucosal layer.		
Fig. 4.3	CT abdomen, sagittal reformatted image showing linitis	39	
	plastica.		
Fig. 4.4	Virtual endoscopic image showing an EGC.	40	
Fig. 4.5	Virtual endoscopic image showing an advanced gastric	41	
	adenocarcinoma.		
Fig. 4.6	Axial CT scan showing a polypoid carcinoma with gross	42	
	infiltration of the perigastric fatty tissue.		
Fig. 4.7	CT abdomen, oblique coronal reformatted image,	43	
	showing a large tumor that protrudes from the posterior		
	wall into the lumen with perigastric and nodal spread.		
Fig. 4.8	CT abdomen, coronal reformatted image of the posterior	43	
	portions of the abdomen shows a large gastric cancer		
	with obliteration of the fat plane and thickening of the		
	colonic wall.		
Fig. 4.9	Coronal reformatted image obtained through the gastric	45	
	fundus shows a T2 gastric cancer of the cardia with		
	multiple lymph nodes.		
Fig. 4.10	CT abdomen, coronal reformatted image showing	46	
	enlarged perigastric and para-aortic lymph nodes and		
T1 444	multiple hepatic metastases.		
Fig. 4.11	CT abdomen, axial cut showing a Krukenberg tumor in a	47	
	patient with known gastric adenocarcinoma.		
Fig. 4.12	CT abdomen, oblique coronal reformatted image shows	48	
	an advanced cancer in the gastric body with ascites and		
	peritoneal carcinomatosis.		
Fig. 4.13	CT abdomen, coronal reformatted image showing greater	48	
	omental infiltration from poorly differentiated		
	adenocarcinoma.		

Fig.4.14(a)	Axial abdominal CT image shows stage T1 gastric	<b>49</b>
_	adenocarcinoma.	
Fig.4.14(b)	Coronal oblique MPR showing stage T2 gastric	<b>49</b>
	adenocarcinoma.	
Fig.4.15(a)	Axial CT of the abdomen showing no lesion.	<b>50</b>
Fig.4.15(b)	MPR image shows no lesions.	50
Fig.4.15(c)	Virtual endoscopic image showing an EGC in the lower	<b>50</b>
	body of the stomach	
Fig.4.15(d)	Conventional endoscopic image showing the EGC.	50
Fig.4.16(a)	Two-dimensional axial CT image of the abdomen	51
	showing no abnormal wall thickening of stomach.	
Fig.4.16(b)	Virtual gastroscopy image shows an EGC.	51
Fig.4.17(a)	Two-dimensional axial abdominal CT image showing an	52
	ECG in prepyloric antrum of the stomach.	
Fig.4.17(b)	Virtual gastroscopy image showing an EGC in prepyloric	<b>52</b>
	antrum of the stomach.	
Fig. 4.17(c)	Conventional gastroscopy image showing an EGC in	52
	prepyloric antrum of the stomach.	
Fig.4.18(a)	Multidetector CT scan of the abdomen, axial cut.	53
Fig.4.18(b)	MPR image.	53
Fig.4.18(c)	Virtual endoscopic image.	53
Fig. 5.1(a)	Multidetector CT scan of the abdomen axial cut.	53
Fig. 5.1(b)	MPR image.	54
Fig. 5.1(c)	Virtual gastroscopy image.	54
Fig. 5.1(d)	Conventional endoscopic image showing type I EGC.	54
Fig. 5.2(a)	Multidetector CT of the abdomen, axial cut.	55
Fig. 5.2(b)	Coronal MPR image.	55
Fig. 5.2(c)	Virtual gastroscopic image.	55
Fig. 5.2(d)	Conventional gastroscopy image showing a type IIc ECG.	55
Fig. 5.3	Transverse dynamic contrast-enhanced CT images show	56
(a-c)	a pathologic stage T1N1gastric cancer in the arterial (a),	
	portovenous (b), and delayed phases (c).	
Fig. 5.3(d)	Coronal MPR shows T1 gastric cancer.	57
Fig. 5.3(e)	Photomicrograph shows submucosal invasion of T1	57
	gastric cancer.	
Fig. 5.3(f)	Virtual gastroscopy image showing elevated lesion at gastr	57
	antrum.	

Fig. 5.2(a)	C1-1111	57
Fig. 5.3(g)	Conventional gastroscopy revealed a similar elevated	51
	ulcerated lesion.	
Fig. 5.4	Coronal oblique arterial phase MPR images show an	<b>58</b>
(a,b)	advanced T3 gastric adenocarcinoma.	
Fig. 5.4(c)	virtual gastroscopy image shows an advanced T3	59
	gastric adenocarcinoma.	
Fig 5.4(d)	conventional gastroscopy image shows an advanced T3	59
	gastric adenocarcinoma.	
Fig. 5.5(a)	Oblique coronal 2D MPR image shows type II advanced	60
	antral gastric cancer.	
Fig. 5.5(b)	Volume-rendered image shows type II advanced antral	60
	gastric cancer.	
Fig. 5.5(c)	Image from virtual gastroscopy shows type II advanced	60
8 ( )	antral gastric cancer.	
Fig. 5.5(d)	Image from conventional gastroscopy shows type II	60
8 ( )	advanced antral gastric cancer.	
Fig. 5.6(a)	Oblique coronal 2D MPR image of the abdomen showing	61
119,000(0)	type III advanced gastric cancer of gastric angle.	01
Fig. 5.6(b)		61
Fig. 3.0(b)	volume rendered image showing type III advanced gastric	O1
	cancer of gastric angle.	
<b>Fig. 5.6</b> (c)	Image from virtual gastroscopy shows type III advanced	61
	gastric cancer of gastric angle.	
<b>Fig. 5.6(d)</b>	Image from conventional gastroscopy type III advanced	61
	gastric cancer of gastric angle.	

# Introduction and aim of the work

## **Introduction**

Despite its declining incidence, gastric cancer remains an important cause of cancer death in Japan and elsewhere (Forman et al, 2000).

To reduce mortality, it is essential to choose an optimal therapeutic approach, and this, in turn, depends on early detection and accurate preoperative staging. Indeed, prognosis is related to the depth of invasion of the gastric wall and lymph node involvement (Msika, 1998).

Survival is improved with curative resection and palliative chemotherapy (**Gill et al, 2003**). A small early gastric cancer confined to the submucosa (T1 stage) can be treated with non surgical endoscopic mucosal resection. Preoperative radiotherapy or chemotherapy is recommended for advanced gastric cancer. Accurate preoperative staging, therefore, can help increase cure rates and quality of life (**Ohashi et al, 1999**).

Preoperative staging has often included endoscopic ultrasonography (US) and computerized tomography (CT), but hydrodynamic helical CT might replace preoperative endoscopic US in (T) and (N) staging (Habermann et al, 2004).

Multidetector row CT with thin collimation offers near-isotropic imaging of the stomach and allows high quality multiplaner reformations (MIPs) and endoluminal three dimensional virtual gastroscopy of gastric images. with adequate distention of the stomach with using water as negative contrast, dynamic contrast material —enhanced CT images offer superior differentiation of tumor tissue from normal mucosa. Also MPRs have advantages for assessing both intra- and extraluminal processes of gastric wall for evaluating more distant regions, such as para-aortic lymph nodes and abdominal organs.

Adding multiplaner reformatted images to transverse CT images also improves the capability of distinguishing T3 from T4 gastric cancer and prediction of adjacent organ invasion (**Kim et al, 2009**).

Contrast enhanced CT can be also used successfully to preoperatively evaluate the staging of remnant gastric cancer in patients who have undergone previous gastric resection (Lee et al, 2010).

<u>The aim of this study</u> is to evaluate the accuracy of multidetector row CT images for preoperative staging of gastric adenocarcinoma.

# Basic and radiological anatomy of the stomach

#### Basic anatomy of the stomach

The stomach is the most distensible organ of the body. It is usually J shaped but varies in size and shape with volume of its contents, with erect and supine position and even with inspiration and expiration (**Ryan and McNicholas, 2004**).

The stomach has two orifices; the cardiac orifice at eosophagogastric junction and the pylorus. It has two curvatures, the greater curvature and lesser curvature. The incisura is an angulation of the lesser curvature. The part of the stomach above the cardia is called the fundus. Between the cardia and incisura is the body of the stomach and distal to incisura is the antrum. The cardiac orifice and the fundus are relatively fixed and only

move with respiratory movement of diaphragm (Fig1.1) (Cunningham and Romanes, 2005).

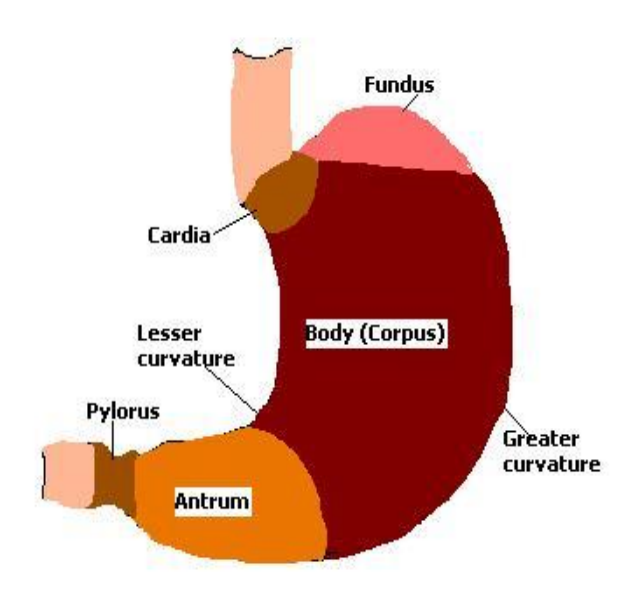


Fig.1.1: Anatomy of the stomach (Quoted from Cunningham and Romanes, 2005)

The stomach passes downward and to the right across the supracolic compartment of peritoneal cavity. It tapers from fundus on the left of median plane to narrow pylorus, 2-3 cms to the right of the median plane. This pyloric part consists of proximal dilated portion, the pyloric antrum and narrow cylindrical portion, the pyloric canal; 2cm long that is continuous distally with the pylorus. The pylorus is the part of the stomach thickened by increase in the amount of circular muscle to form the pyloric sphincter that controls the rate of discharge of the stomach content into the duodenum (Fig. 1.2) (Cunningham and Romanes, 2005).

The pylorus is highly mobile because the omentum is attached to it. It may lie anywhere between the first and the third lumbar vertebrae. It is further transferred to the right when the stomach is full. In its higher position the pylorus is posterior to the quadrate lobe of the liver and is separated from the pancreas by the omental bursa (**Cunningham and Romanes**, 2005).

The fundus abuts on the left dome of diaphragm under the cover of the rib cage and reaches the level of the fifth rib in the midclavicular line anteriorly. The cardiac orifice lies approximately 10 cm posterior to the seventh left costal cartilage, 2-3 cm from the median plane between the liver and the diaphragm (Cunningham and Romanes, 2005).

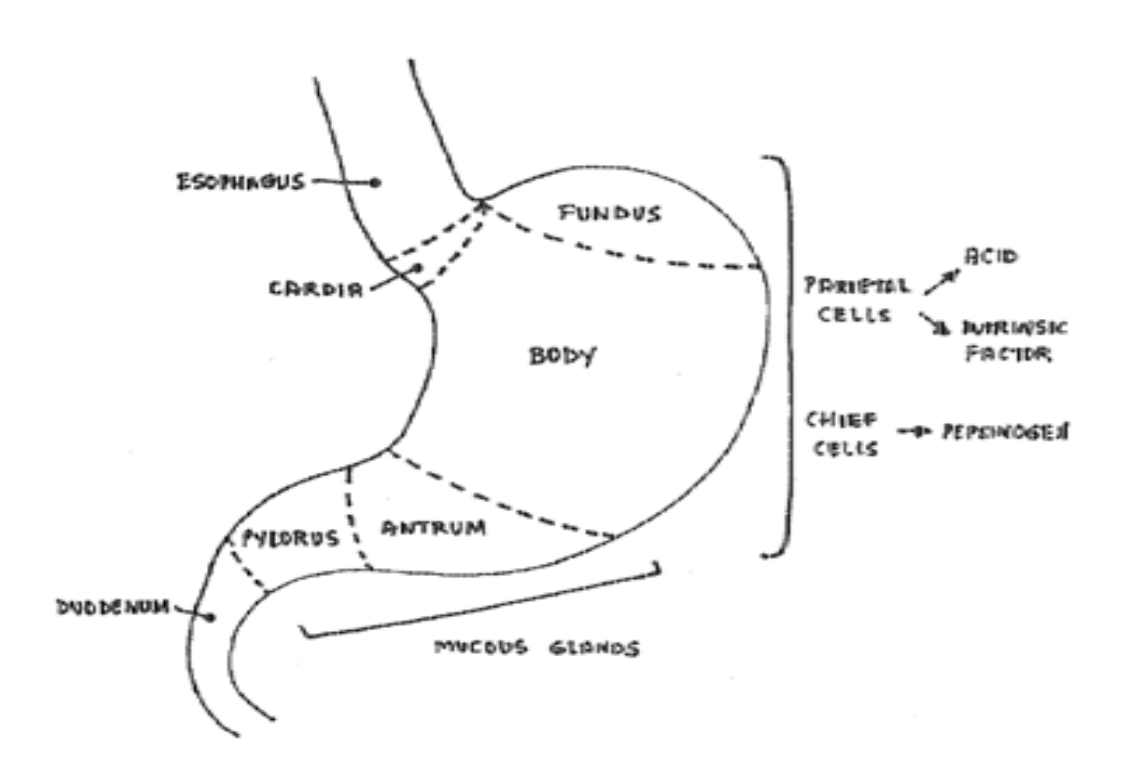


Fig. 1.2: Anatomy of the stomach (Quoted from Ryan and McNicholas, 2004)

The stomach is lined by mucosa that is tiny nodular elevations called the area gastrica and is thrown into folds called rugae. The longitudinal folds parallel to the lesser curvature called magenstrasse; rugae elsewhere in the stomach are random and patternless (**Ryan and McNicholas, 2004**).

There are three muscle layers in the wall of the stomach, an outer longitudinal, inner circular and incomplete innermost oblique layer (**Fig. 1.3**). The circular layer is thickened at the pylorus as a sphincter but not at esophagogasteric junction. Fibers of oblique layer loop around the notch between the fundus and esophagus and help to prevent reflux (**Ryan and McNicholas, 2004**).

The upper part of the anterior surface of the stomach is covered by the left lobe of the liver on the left and by the diaphragm on the right. The fundus occupies the left dome of the diaphragm. The abdominal wall covers the remaining part of the anterior wall of the stomach (**Fig. 1.4**). Posterior to the stomach lies the lesser sac, the structures of the posterior abdominal wall that are posterior to this, are referred to as the stomach bed. The pancreas lies across the mid-portion of the stomach bed with the splenic artery partly above and partly behind it, and the spleen at its tail. Above the pancreas are the aorta and its coeliac trunk and the surrounding plexus and nodes, the diaphragm, the left kidney and left adrenal gland. Attached to the anterior surface of the pancreas is the transverse mesocolon which forms the inferior part of the stomach bed (**Fig. 1.5**) (**Ryan and McNicholas, 2004**).

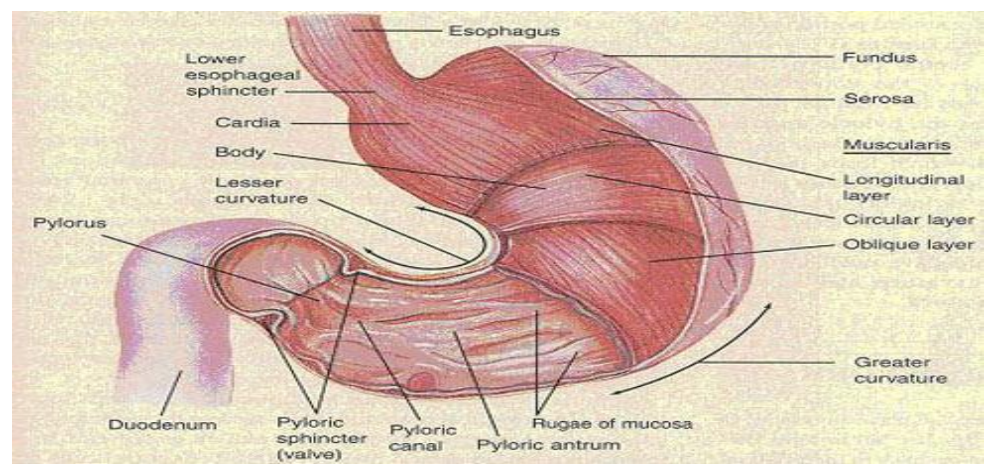


Fig. 1.3:muscle layers of the stomach(Quoted from Tortora and Grabowski, 2002).

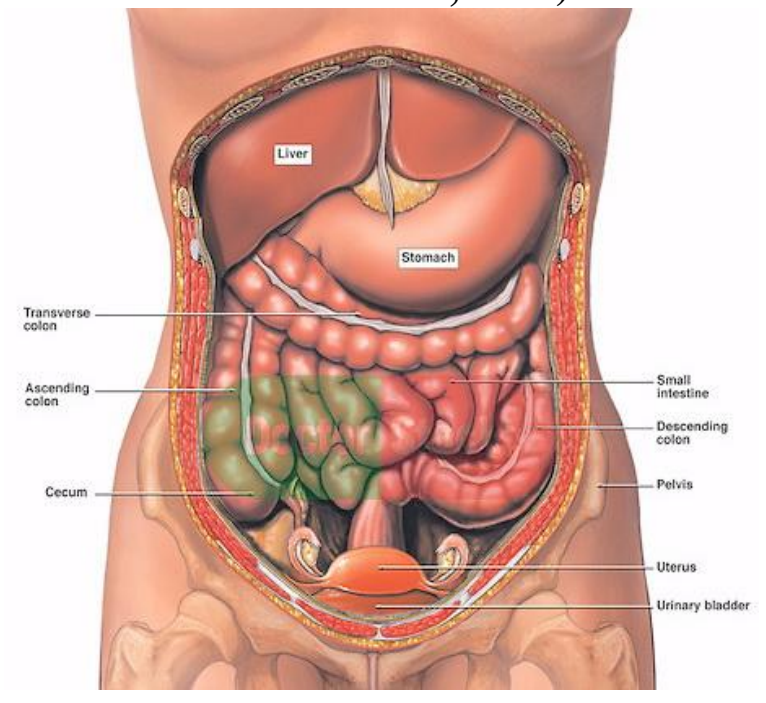


Fig. 1.4: Relations of the stomach (Quoted from Doctor Stock, 2012)